Absolute band-structure determination by target current spectroscopy: Application to Cu(100)

V. N. Strocov* and H. I. Starnberg
Department of Physics, Chalmers University of Technology and Göteborg University, S-412 96 Göteborg, Sweden
(Received 3 April 1995)

Experimental data obtained by application of target current spectroscopy (TCS) to the Cu(100) surface are presented, and used for absolute mapping of unoccupied electronic bands, i.e., without requiring knowledge about any other bands. A simple scheme for data analysis which yet allows for accurate band mapping was used. All features observed in the experiment could be identified as due to either the bulk band structure, or to surface-barrier resonances. Good agreement with *ab initio* band-structure calculations was found. The potential of TCS for band mapping and for studies of excited states are discussed, emphasizing the need for appropriate calculational schemes.

I. INTRODUCTION

The most important concept for the understanding of the physical properties of crystalline solids is undoubtedly the electronic band structure. The most widely used methods for obtaining detailed information about the occupied and unoccupied electronic bands are photoemission spectroscopy (PES) and inverse photoemission spectroscopy (IPES), respectively. A fundamental limitation associated with these methods is that they both exploit processes involving two states: In PES, transitions occur from states below the Fermi level E_F to states above, while in IPES transitions occur from higher to lower states which are all above E_F.

By using PES in its angle-resolved mode (ARPES) one easily determines energies of occupied electronic states as functions of $\mathbf{k}_\parallel$, the wave-vector component parallel to the surface. But also to obtain the perpendicular components $k_\perp$ one needs additional information about the final states involved. In principle, unoccupied states can also be determined by ARPES, but beforehand knowledge about the initial states is required in such cases.

A particular advantage of IPES is the possibility to probe states between E_F and the vacuum level, but again a full wave-vector determination requires knowledge about the higher states from which the electrons are deexcited.

Different approaches have been used to circumvent this problem, but a particularly straightforward solution is offered by using the band-structure information provided by low-energy electron diffraction (LEED) and related methods, since in these only one electronic state is involved.[1–4] Two closely related methods for obtaining this information are very-low-energy electron diffraction (VLEED) and target (or total) current spectroscopy (TCS).[5–8] Both methods employ an electron beam of kinetic energy E, typically is in the range 0–30 eV, directed onto a sample surface, and in VLEED the elastically reflected current is measured as a function of E, while in TCS the absorbed (transmitted) current is measured. The transmission T is related to the reflectivity by

$$T=1-R_e-R_i\ , \tag{1}$$

where R_e and R_i are the elastic and inelastic reflectivities. R_i represents reflected electrons which have undergone energy-loss processes, but it also contains a contribution due to emission of secondary electrons. Although dependent on the kinetic energy of the primary beam, R_i usually varies slowly, so that TCS data essentially contain the same information as R_e obtained from VLEED measurements. From an experimental point of view, TCS has the advantage of being more convenient to apply than VLEED, although the results can be analyzed by the same means.

Apart from band-structure features, $R_e(E)$ and $T(E)$ may also exhibit narrow oscillations due to surface resonances.[9,10] These oscillations are known to converge toward the threshold $E=\hbar^2(\mathbf{K}_\parallel+\mathbf{g})^2/2m$, where an additional diffracted beam appears, and are caused by interference between the specularly reflected beam, and preemergent diffracted beams traveling along the surface via multiple reflections between the substrate and the surface barrier. Since elastic damping is weak in the barrier region, these features are narrower than those related to the bulk bands.

There is a close connection between PES and IPES on one hand, and LEED on the other, because in terms of one-step photoemission theory the higher states involved in PES and IPES are LEED states, of the same kind as those excited in a VLEED or TCS experiment.[11]

One way in which TCS data can be used is to carry out full calculations from first principles, and to verify these calculations by comparison between calculated and measured spectra. Possibly a few free parameters in the calculational scheme can be varied as to obtain the closest agreement possible. In a sense, these parameters are then determined from experiment, on the condition that the theoretical model used is physically sound. The approach favored by us is to use a procedure for band mapping point by point, where an approximate calculational scheme is used as a guide, but where extreme accuracy is not required in the calculations.

In this work we demonstrate how a conventional LEED unit, of the kind available on most UHV systems used in surface science, may be utilized for band mapping by TCS. We have applied the technique to the Cu(100)

0163-1829/95/52(12)/8759(7)/$06.00

surface, which has been thoroughly studied by different methods, and which is theoretically well understood. For these reasons Cu(100) is well suited as a testing ground for TCS. We also demonstrate the necessity of adequate calculations in order to interpret the data correctly. The band mapping is carried out starting from an approximate band structure and VLEED calculation, which is corrected with use of the experimental TCS data. A very important advantage of this kind of semiempirical band mapping is that time-saving approximate methods can be used for the calculations, without compromising the accuracy of the final band mapping.

II. EXPERIMENTAL DETAILS

We have measured VLEED spectra by the TCS method, using a conventional LEED Auger unit (PHI 15-120). When analyzing and presenting TCS data it is preferable to work with the first derivative dT/dE, rather than with the transmission T itself, as the dT/dE maxima and minima can be directly associated with band edges and similar features of the band structure. Differentiation also enhances the spectral fine structure, while suppressing the inelastic background. The dT/dE curves were obtained by numerical differentiation of the measured absorbed current. A retarding field between the electron gun and sample was produced by biasing all grids (and the gun drift tube) to $+100$ V. This retarding field swept away all secondary electrons and enabled measurements down to zero kinetic energy.[8,12] The electrons left the gun with energies in excess of 100 eV, and were retarded to very low kinetic energy as they approached the sample. A special advantage of the experimental geometry is that most of the retardation takes place in the immediate proximity of the sample. Such conditions are favorable for efficient operation of the gun, and minimize the influence of stray magnetic and electrostatic fields. In addition, magnetic fields were suppressed by means of mu-metal screening and external Helmholz coils. The sample was kept as close as possible to the electron gun exit, and a well-focused beam was obtained over the whole 0–35-eV primary energy range. The primary beam current was typically kept at 1 μA, as larger currents degraded the focusing. As an upper limit for the energy spread of the beam, we may take the width of the first dT/dE peak (corresponding to the onset at zero kinetic energy), which was 0.8 eV [full width at half maximum (FWHM)].

When the sample is rotated, the retarding field deflects the incident electrons, thereby increasing the incidence angle.[13] The deflection is larger the smaller the primary energy is. This effect reduces the variation of $\mathbf{K}_{\parallel}$ along any experimental spectrum.[12,14] In principle $\mathbf{K}_{\parallel}$ should vary less over the spectral range (0–30 eV in our case) the higher the bias voltage is, but we chose $+100$ V, since higher voltages resulted in unacceptable disturbances of the electrons trajectories (caused by protruding manipulator parts at the ground potential).

The Cu(100) sample was cleaned *in situ* by standard ion bombardment and annealing. Once the surface was thoroughly cleaned, overnight contamination could be removed by flash heating. The surface cleanliness was monitored by the dT/dE spectra themselves, as these are much more sensitive to contamination than, e.g., Auger electron spectra.[8,12] An additional indication of high surface purity and negligible roughness was the appearance of surface resonance structures.

The incidence angle was set by rotating the sample around the vertical axis. The normal-incidence orientation was easily found by using the strong angular dependence of dT/dE spectra.[12,15] Due to the symmetry of the Cu(100) surface, normal incidence corresponds to extremal energies of spectral features. The normal-incidence orientation was easily determined by searching for the maximum energy of the spectral features at about 25 eV. We observed that the setting also minimized the energy of target current onset.

The approximate azimuthal orientation was set by visual inspection of the diffraction pattern. An accurate setting was thereafter found by watching for extremal spectral behavior upon variation of the azimuthal orientation. Due to the symmetry of the surface Brillouin zone, such extremal spectra indicate either $\overline{\Gamma X}$ and $\overline{\Gamma M}$ azimuthal directions.

Although the strong angular dependence of our dT/dE spectra in principle allows for sample alignment with high accuracy ($\pm 0.5°$), the sample holder geometry used by us (main rotation around a vertical axis plus azimuthal rotation around an axis in the horizontal plane) prevented us from eliminating a residual vertical deviation (1°–2°) between the surface normal and the beam. In principle, such a vertical misalignment will result in deviations from the symmetry lines of the surface Brillouin zone as $\mathbf{K}_{\parallel}$ varies. Deviations from the correct symmetry planes will lift the degeneracy of related bands, and result in splitting of spectral features. The fact that our measured spectra do not show appreciable splittings shows that the misalignments were minor.

III. EXPERIMENTAL RESULTS

The dT/dE spectra measured with electron incidence scanning along the $\overline{\Gamma M}$ and $\overline{\Gamma X}$ azimuthal directions are presented in Figs. 1(a) and 1(b), respectively. The spectra exhibit a profusion of features, which are all strongly dependent on the incidence angle. Of the possible inelastic processes, electron interband transitions will reflect surface or bulk density of states, and the corresponding spectral features should therefore not depend appreciably on the incidence angle.[8] Neither should any other inelastic processes (e.g., plasmon excitations) show a pronounced angular dependency. The observed dispersion therefore verifies that all spectral features are of elastic origin.

The dominant features in Fig. 1 are rather broad (widths >2 eV). They are connected by dashed lines and labeled $A-G$ with superscripts $+$ or $-$ depending on if they appear as maxima or minima. By comparison with band-structure-based calculations, we show below that they are associated with well-defined critical points (CP's) of bands (such as band-gap edges). Some features are due

to CP's in the interior of the Brillouin zone (BZ), while others are due to CP's along symmetry lines. Only the latter ones are useful for band mapping along symmetry lines.

Our measured dT/dE spectra also exhibit narrow (widths <1 eV) oscillations which we attribute to surface resonances.[9,10,16] Apart from their narrowness, they are also characterized by parabolic $\mathbf{K}_{\parallel}$ dispersion, and convergence toward the diffraction thresholds. At more glancing incidence angles, these features become sharper and more prominent, because the electrons are then penetrating less into the bulk, and consequently experience less absorption. In Fig. 1 the surface resonances are indicated by dotted lines and labeled by the surface reciprocal vector $\mathbf{g}$ of their associated diffracted beam.

IV. CALCULATIONS OF dT/dE

Our analysis of the TCS data is based on the matching approach of LEED theory.[1,2] The periodicity of the surface implies that the impinging electrons will only couple to Bloch states having the same reduced wave-vector component parallel to the surface, i.e., states with $\mathbf{k}_{\parallel}=\mathbf{K}_{\parallel}+\mathbf{g}$, where $\mathbf{K}_{\parallel}$ is the parallel wave-vector component of the impinging electron, and $\mathbf{g}$ is any surface reciprocal-lattice vector. The Bloch states along these lines in $\mathbf{k}$ space determine, through the matching on the surface, the amplitude of the reflected wave. For example, if for a given E and $\mathbf{K}_{\parallel}$ there are no states available, all electrons will be reflected back by the surface (neglecting inelastic processes). Near CP's of the band structure (such as band-gap edges) Bloch states undergo drastic changes, which produce drastic changes of $T(E)$. If now the derivative dT/dE is recorded in the experiment, such CP's will show up as minima or maxima in these spectra.[3,4,17]

Because of inelastic broadening and the multitude of bands involved, reference calculations are necessary in order to determine which CP's are responsible for the observed experimental dT/dE features. For a given $\mathbf{K}_{\parallel}$ one

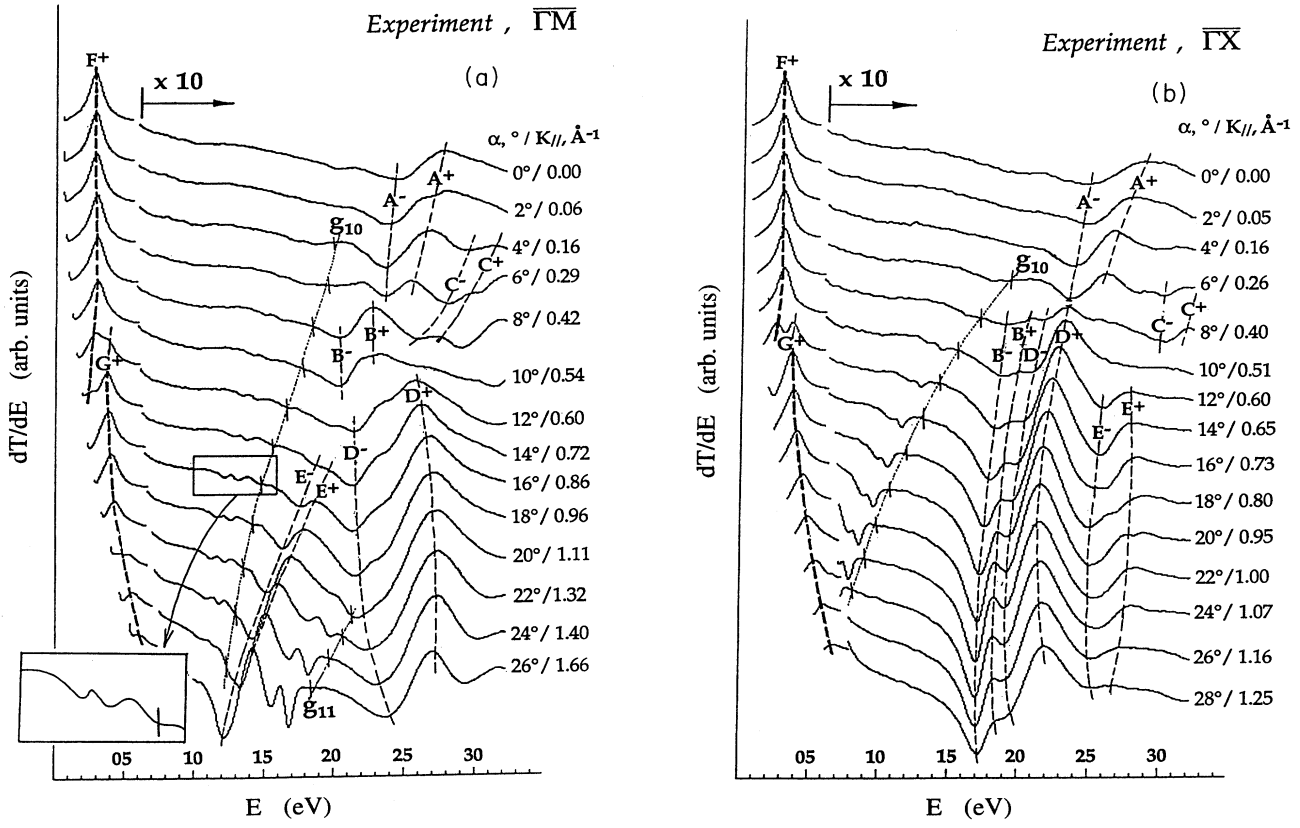

FIG. 1. Experimental dT/dE spectra recorded in (a) the $\overline{\Gamma M}$ and (b) the $\overline{\Gamma X}$ azimuthal directions. For each spectrum is given the sample rotation angle α and the extrapolated value of $K_{\parallel}$ at $E=20$ eV. The features due to the bulk band structure are connected with dashed lines and designated with letters $A-G$, with superscripts $-$ for minima, and $+$ for maxima. The dashed lines corresponding to bands along XW ($\overline{\Gamma M}$) and ΓKX ($\overline{\Gamma X}$) are drawn bolder. The large peaks at $E=\hbar^2\mathbf{K}_{\parallel}^2/2m$ due to the current onset are excluded from the figure. The spectra are magnified by a factor of 10 for energies above the first peak F^+. The diffraction thresholds giving rise to surface resonances are indicated by dotted lines, and labeled by the relevant $\mathbf{g}$ vector. The inset shows the surface resonance oscillation in magnification.

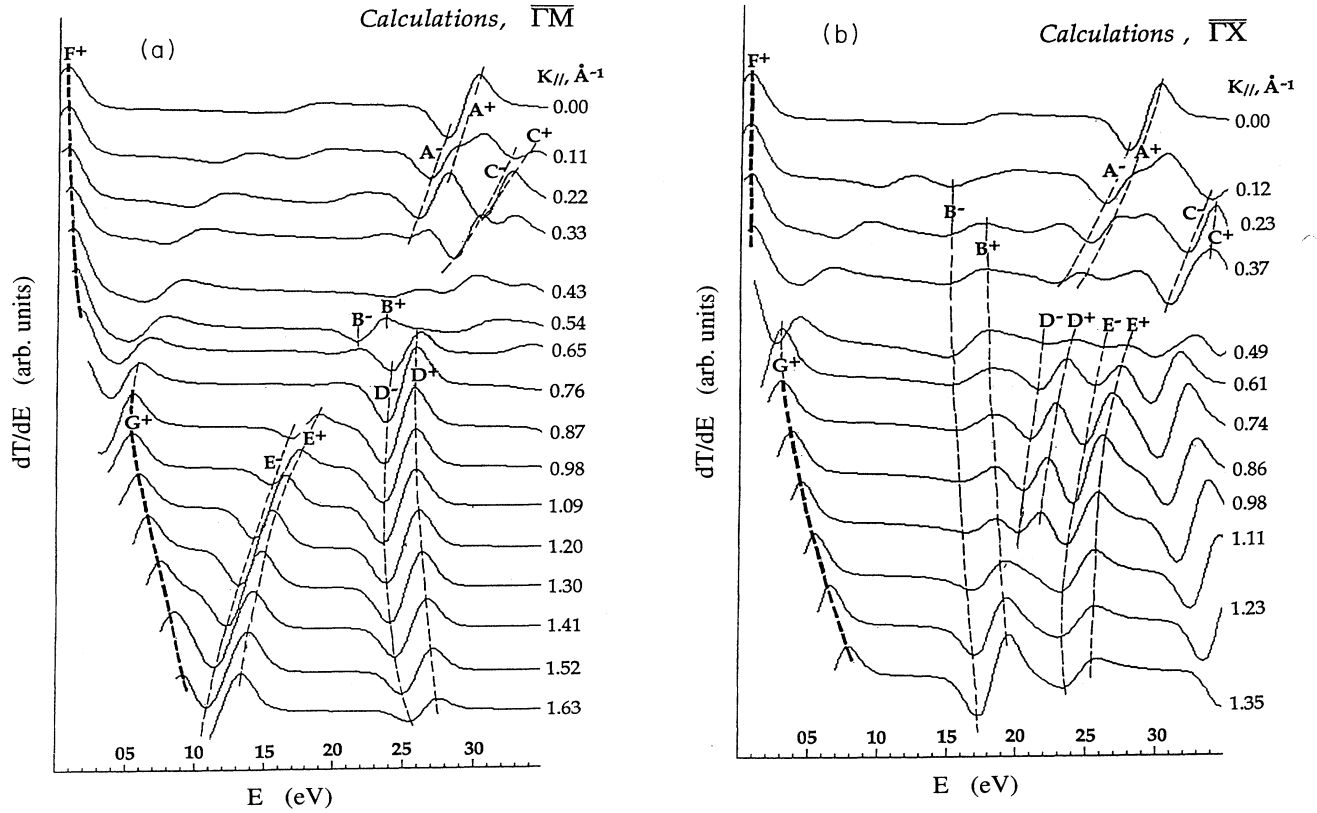

FIG. 2. Calculated dT/dE spectra for (a) the $\overline{\Gamma M}$ and (b) the $\overline{\Gamma X}$ azimuthal directions. The accuracy is 0.125 eV. The features are labeled in agreement with their experimental counterparts in Fig. 1, and the maxima connected by bold dashed lines are those corresponding to bands along XW ($\overline{\Gamma M}$) and ΓKX ($\overline{\Gamma X}$).

may calculate the band structure along the corresponding lines in the reduced zone. We have used an empirical pseudopotential scheme for this purpose, and the associated dT/dE spectra were calculated by the fast approximate conducting Fourier component (CFC) method,[3,12] neglecting surface barrier reflection. In a plane-wave expansion of bulk band states, the CFC is the Fourier component $\exp[i(\mathbf{k}+\mathbf{G})\cdot\mathbf{r}]$ which is matched to the primary plane wave $\exp[i\mathbf{K}\cdot\mathbf{r}]$ through the relation $\mathbf{k}_\parallel+\mathbf{G}_\parallel=\mathbf{K}_\parallel$. The transmission $T(E)$ is related to the CFC amplitude $C_{\mathbf{k}_\parallel+\mathbf{G}_\parallel=\mathbf{K}_\parallel}$ through a semiempirical function $T(E)=F[C_{\mathbf{k}_\parallel+\mathbf{G}_\parallel=\mathbf{K}_\parallel}(E)]$. The inelastic broadening was simulated by Gaussian convolution with the optical potential $V_i=1$ eV.

The calculated dT/dE spectra are presented in Fig. 2 with minima and maxima labeled analogously to the corresponding experimental features in Fig. 1.

V. DATA ANALYSIS AND DISCUSSION

Since the calculations are based on the bulk band structure, they do not reproduce the surface resonance oscillations. It should also be pointed out that each dT/dE spectrum in Fig. 2 was calculated for a constant $\mathbf{K}_\parallel$, while each experimental spectrum in Fig. 1 refers to a specific orientation of the sample, with $\mathbf{K}_\parallel$ somewhat dependent on E. Other discrepancies between experimental and calculated spectra are expected due to the inaccuracy of the pseudopotential used, and the approximations made when calculating dT/dE by the CFC method. The optical potential at higher energies is most likely underestimated. Finally some differences may be due to experimental errors. For example, the noticeable splitting in Fig. 1(a) around 24 eV ($\alpha=10°-20°$, $\overline{\Gamma M}$ azimuth) can be attributed to sample misalignment, which puts $\mathbf{K}_\parallel$ slightly off the symmetry azimuth. Highly dispersive features may be suppressed by the divergence of the primary beam.

One can notice a weak minimum-maximum structure in the normal-incidence dT/dE curves of Fig. 1 near 20 eV. On Ni, a similar feature was explained as a strong-overlap surface resonance[18] which is broader than an ordinary surface resonance because its wave function penetrates more deeply into the solid. We instead associate this structure with a calculated feature near 18 eV, which is due to a hybridization band gap between two Δ_1 bands in the BZ interior. A combination of both kinds of contributions is also possible.

Still, apart from the surface resonances, the experimental features of dT/dE are well reproduced by the calculations, with regard to their amplitudes as well as to their dispersions. It is evident, from the agreement found, that all significant features are due to either surface resonances or the bulk band structure. The lack of features

produced by inelastic scattering justifies the analysis of TCS data by elastic VLEED calculations, at least on Cu.

As mentioned above in Sec. II, the bias +100 V is too small to ensure $\mathbf{K}_{\parallel}$ conservation. By calculating electron trajectories, assuming asymptotic spherical symmetry for the field away from the sample, we found that an increase of $\mathbf{K}_{\parallel}$ by 21% can be expected as the kinetic energy is scanned from 5 to 35 eV. The calculations also predicted $\mathbf{K}_{\parallel}$ to be highly sensitive to residual misalignments and stray fields, in particular for energies below 10–15 eV. It turned out that $\mathbf{K}_{\parallel}$ could be determined more accurately by empirical methods: In each spectrum, the first point with well-defined $\mathbf{K}_{\parallel}$ is the target current onset, where the energy becomes sufficient for electrons to penetrate into the sample. There $\mathbf{K}_{\parallel}$ is obtained from the relation $E=\hbar^2\mathbf{K}_{\parallel}^2/2m$. Other points with well-defined $\mathbf{K}_{\parallel}$ are those where a diffracted beam emerges. These points are the ones toward which the surface resonance oscillations converge, and $\mathbf{K}_{\parallel}$ can be found using that $E=\hbar^2(\mathbf{K}_{\parallel}+\mathbf{g})^2/2m$, $\mathbf{g}$ being the associated surface reciprocal vector. Between the target current onset and the diffraction thresholds, $\mathbf{K}_{\parallel}$ was obtained by linear interpolation, with an uncertainty of 2–3 %.

Having found the experimental $\mathbf{K}_{\parallel}$ with satisfactory accuracy, the next step is to relate every experimental extremum of dT/dE to a specific CP. This is easily done with the assistance of the reference calculations, as is illustrated in Fig. 3 (for the case $\mathbf{K}_{\parallel}=1.195$ Å^{-1}, $\overline{\Gamma M}$ azimuth). Throughout the multitude of bands, dT/dE extrema are produced only by CP's of bands which are matched with the incident plane wave, $\exp[i\mathbf{K}\cdot\mathbf{r}]$. As mentioned above, this is the case if a band has a leading component which satisfies $\mathbf{k}_{\parallel}+\mathbf{G}_{\parallel}=\mathbf{K}_{\parallel}$.[3,19] Utilizing the Fourier expansion generated by the calculations, one may identify such bands (indicated by bold lines in Fig. 3). The other bands are not significantly excited, and do therefore not contribute to dT/dE.

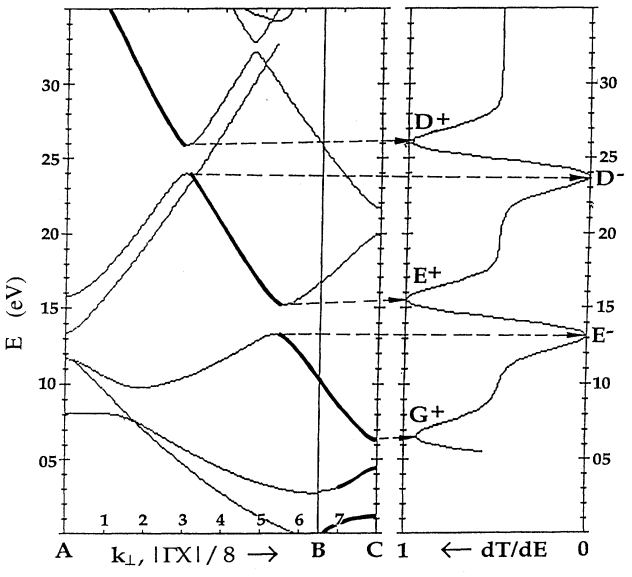

FIG. 3. Calculated reference bands along $\mathbf{k}_{\parallel}=\mathbf{K}_{\parallel}$ (from A to B), and $\mathbf{k}_{\parallel}=\mathbf{K}_{\parallel}+\mathbf{g}_{10}$ (B–C) for $K_{\parallel}=1.195$ Å^{-1} in the $\overline{\Gamma M}$ azimuth. The bands which are strongly coupled to incident plane waves are drawn with bold lines. The corresponding calculated dT/dE spectrum is shown to the right. The dT/dE extrema are connected with the associated CP's by arrows.

We may distinguish between two different kinds of CP's. The first kind is found where the $\mathbf{k}_{\parallel}=\mathbf{K}_{\parallel}+\mathbf{g}$ lines cross perpendicular symmetry planes, e.g., ΓXWK or XWU planes in the present case. As $k_{\perp}$ is well defined on these planes, such CP's are particularly useful for band-mapping purposes. The other kind of CP's are due to hybridization band gaps in the interior of the BZ, and $k_{\perp}$ is not well defined by k-space geometry. It is clear from Fig. 3 that the extrema labeled E^-, E^+, D^-, and D^+ correspond to interior CP's, while G^+ is due to a CP in the ΓXWK plane. By this kind of analysis we found that, of all CP signatures seen in our dT/dE spectra, only the F^+ and G^+ features (for both $\overline{\Gamma M}$ and $\overline{\Gamma X}$ azimuth) correspond to symmetry plane CP's. For this reason these features are indicated by bold dashed lines in Figs. 1 and 2.

For the measurements with $\mathbf{K}_{\parallel}$ in the $\overline{\Gamma M}$ azimuth, we found that the CP corresponding to F^+ was located in the intersection of the line $\mathbf{k}_{\parallel}=\mathbf{K}_{\parallel}$ with the XWU plane, and followed the lower Z_1 band along the XW line. As $\mathbf{K}_{\parallel}$ exceeded the XW distance, F^+ disappeared from the dT/dE curves, and instead G^+ emerged, corresponding to a CP in the intersection of the umklapp line $\mathbf{k}_{\parallel}=\mathbf{K}_{\parallel}+\mathbf{g}_{10}$ with the ΓXWK plane, which scans the upper Z_1 band along the XW line.

In the $\overline{\Gamma X}$ azimuthal, F^+ correspond to a CP which follows the S_1 band from X to U in the XWU plane, while the umklapp feature G^+ maps the Σ_1 band from K to Γ. To determine the energy of the experimental CP's we first determined how much the calculated dT/dE features have to be shifted in energy to coincide with their experimental counterparts. The experimental CP energies were thereafter obtained by shifting the corresponding calculated energies by the same amount. This way we found, throughout the entire $\mathbf{K}_{\parallel}$ range, the energies of the CP's giving rise to F^+ and G^+.

The CP's corresponding to F^+ and G^+, and located in $\mathbf{k}$ space where $\mathbf{k}_{\parallel}=\mathbf{K}_{\parallel}+\mathbf{g}$ lines intersect ΓXWK or XWU symmetry planes, are mainly found outside the irreducible wedge of the BZ. By folding the experimental bands to standard symmetry lines, we obtained the experimental band structure as presented in Fig. 4. The experimental points are superimposed on bands produced by a self-consistent linearized augmented plane-wave (LAPW) calculation,[20] using a parametrized exchange-correlation potential.[21] The experimental energies are accurate to within about ±0.25 eV, while values of $\mathbf{K}_{\parallel}$ are determined accurately within ±0.02 to ±0.04 Å^{-1}.

The final result presented in Fig. 4 shows the feasibility of TCS as an independent method for band mapping. The experimental points are in reasonable overall agreement with the LAPW calculation. However, the experimental data definitely reveal band gaps between the two Σ_1 (S_1) bands along ΓKX, and between the two Z_1 bands

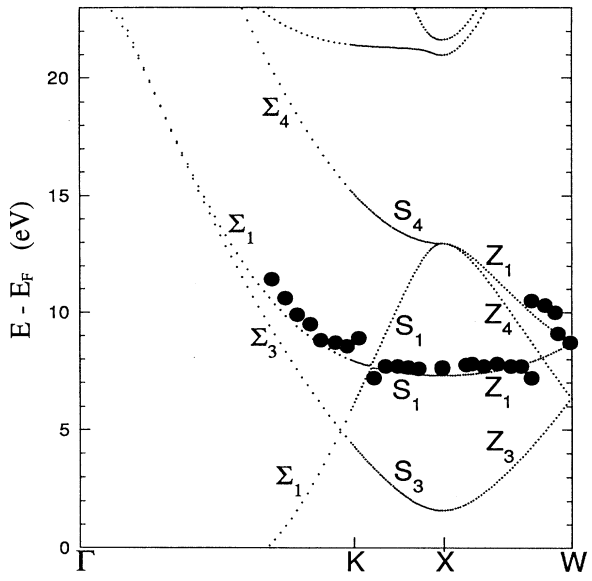

FIG. 4. The experimental points along ΓKX and XW, which are obtained from the dT/dE spectra in Figs. 1(a) and 1(b), respectively. The size of the experimental points are approximately in accordance with the experimental inaccuracy. The superimposed bands (dotted lines) were calculated by the LAPW method.

along XW, which are not seen in the LAPW calculations. Most likely this is an artifact of the LAPW calculation, because bands of the same symmetry should interact in the presence of the crystal potential, to produce such gaps. In fact, these band gaps are apparent in other band-structure calculations.[22] Possibly the experimental band gaps are somewhat exaggerated due to misalignments, which may put $\mathbf{K}_{\parallel}$ slightly off the correct azimuthal directions.

In principle, a crude understanding of TCS data could be gained from just plotting dT/dE maxima and minima against $K_{\parallel}$, together with calculated bands along appropriate symmetry planes (with well-defined $k_{\perp}$). The main problem here would be that association of spectral features with the calculated bands would be confused by TCS features produced by interior CP's. In the present case such features outnumber those associated with symmetry-plane CP's, but in other systems (e.g., layered materials) this may be a lesser problem. Furthermore, such an analysis would be inaccurate, because the vanishing electron group velocity at the extremal points and the inelastic smoothing both tend to shift the dT/dE maxima and minima away from the corresponding CP energies.[23]

It is obvious from the analysis of the data that appropriate VLEED calculations are absolutely necessary in order to interpret the measured dT/dE curves correctly. Basically three crucial questions are answered by the calculations: (1) Which CP's produce significant dT/dE spectral features? (2) Which CP's are located on symmetry planes in $\mathbf{k}$ space? (3) How large is the energy difference between each CP and its corresponding spectral maximum or minimum? Our study shows that accurate results can be obtained even with fast approximate methods, but application of first-principles LEED calculations may of course improve the precision further. As a full calculation invoking the potential barrier at the surface should reproduce surface resonance features, it would also be useful for studies of surface barriers.

Although most observed spectral features are due to CP's not located on perpendicular symmetry planes in $\mathbf{k}$ space, they still carry useful information about the band structure. We found that variations in the pseudopotential of our approximate band calculations only produced negligible changes in the values of $k_{\perp}$ obtained for interior CP's. This means that these CP's can also be quite accurately determined, and that they are consequently useful for verification of band-structure calculations, or as input in band-fitting schemes.

From a strict point of view, VLEED probes excited electronic states, while band calculations normally refer to the ground state.[24] In excited-state calculations one has to include the inelastic scattering and finite lifetime of states away from E_F, and both E and $\mathbf{k}$ become complex entities. When excited-state bands are plotted (as Re E versus Re $\mathbf{k}$), one typically finds continuous lines closing the gaps of the ground-state band structure.[1,23] Considering this it may seem surprising that all major band-structure features of the experimental spectra (Fig. 1) are so well reproduced by calculations (Fig. 2) based on the ground-state band structure. It seems, however, that this closing of band gaps is not very relevant, at least from a VLEED point of view. Although bulk states are introduced in the gaps, these states are characterized by such large values of Im $\mathbf{k}$ that they are not efficient in transporting the electrons. One may say that an effective band gap remains, for which the edges of the ground-state bands are replaced by the inflection points of the complex excited-state bands.[4,23] Since the self-energy corrections are not very pronounced in the VLEED range, these inflection points do not differ appreciably from the ground-state CP's and result in more or less the same dT/dE extrema.

However, there is a possibility that some of the band-gap enhancement seen when comparing mapped bands to LAPW calculations (e.g., for S_1-S_1 and Z_1-Z_1 gaps in Fig. 4) is due to an excited-state effect: In contrast to the gap edges of the ground-state bands, the corresponding inflection points of the excited-state bands are somewhat displaced from the symmetry lines, toward the BZ interior, thereby lifting symmetry degeneracies. From the ground-state point of view, this may result in effectively wider band gaps. To resolve this issue, further calculations based on the excited-state approach are required.

It is interesting to note that, compared to the ground-state bands, excited-state bands appear to be more free-electron-like. This fact is often used to justify the free-electron approximation for them. However, the features of dT/dE provide strong evidence of drastic changes in the composition of band states at inflection points, and these changes are clearly beyond the free-electron approximation.

It should be pointed out that the similarity between upper PES states and LEED states is violated when electron/hole interactions are accounted for, because in PES there is a hole present which is not involved in LEED states. This fact can possibly be exploited in studies of excited-state effects. The similarity between upper IPES states and LEED states remains, however, as in both cases an electron is added to the system under study. The results obtained here are consistent with those previously obtained from other Cu and Ni surfaces.[12,19]

VI. CONCLUSIONS

We have studied the unoccupied band structure of Cu by TCS, and demonstrated how this method can be utilized for absolute band mapping above the vacuum level. As the method provides information complementary to that obtained by PES and IPES, with modest experimental requirements, it has potential for widespread use in the future.

All structures seen in experimental dT/dE spectra can be understood as either bulk band signatures or surface resonance oscillations. The strong angular dispersion of all spectral features excludes significant contributions from inelastic processes.

Fairly good agreement was found between our TCS mapped bands and a self-consistent LAPW calculation. Of the deviations observed, some could be attributed to inaccuracy of the LAPW band structure, while others are more likely due to a small experimental misalignment. A third possibility is that excited-state effects lead to an increased virtual splitting of adjacent bands.

Our results show that the use of an appropriate calculational scheme is of utmost importance, in order to interpret the spectra correctly. However, with the approach taken by us it is possible to map bands accurately even with an approximate calculational scheme. The scheme used by us is well suited for fcc metals, and its extension to other structures is straightforward. Alternative schemes may be developed that refines accuracy further, or which are better suited for more complicated structures, and by inclusion of model surface barriers in the scheme one may extract more information about the surface electronic structure.

We have found a close relationship between TCS data and the ground-state band structure, despite the closing of band gaps suggested by excited-state calculations. The reason for this seems to be that the states in these closed gaps decays too quickly to support any significant transport of the incident electrons. From an electronic transport point of view an effective gap remains, with the ground-state gap edges replaced by the inflection points of the excited-state bands. Although the real parts of excited-state bands may look very free-electron-like, the free-electron approximation is not justified in general.

A particularly interesting development would be to achieve a better understanding of excited-state effects. TCS should be a useful technique in such studies, and in the end additional insights may benefit the analysis of TCS data considerably.

The most significant advantage of the present data, as compared to other methods, is that the upper states were obtained without assumptions about any other states. This can be exploited in (inverse) photoemission investigations for determination of lower bands.

ACKNOWLEDGMENTS

This work has been supported by the Swedish Natural Science Research Council and by the Royal Swedish Academy of Science through a travel grant.

*On leave from Int. Inst. of Interphase Interactions, P.O. Box 1146, St. Petersburg 194291, Russia.

[1]J. B. Pendry, *Low-Energy Electron Diffraction* (Academic, London, 1974).
[2]G. Capart, Surf. Sci. **13**, 361 (1969).
[3]V. N. Strocov, Solid State Commun. **78**, 545 (1991).
[4]V. N. Strocov, Int. J. Mod. Phys. B (to be published).
[5]I. Schäfer, M. Schlüter, and M. Skibowski, Phys. Rev. B **35**, 7663 (1987).
[6]A. Otto, B. Reihl, Phys. Rev. B **41**, 9752 (1990).
[7]R. Drube, J. Noffke, R. Schneider, J. Rogizik, and V. Dose, Phys. Rev. B **45**, 4390 (1992).
[8]S. A. Komolov, *Total Current Spectroscopy of Surfaces* (Gordon and Breach, Philadelphia, 1992).
[9]E. G. McRae, Rev. Mod. Phys. **51**, 541 (1979).
[10]R. O. Jones and P. J. Jennings, Surf. Sci. Rep. **9**, 165 (1988).
[11]J. F. L. Hopkinson, J. B. Pendry, and D. J. Titterington, Comput. Phys. Commun. **19**, 69 (1980).
[12]V. N. Strocov and S. A. Komolov, Phys. Status Solidi B **167**, 605 (1991).
[13]A. Dittmar-Wituski, M. Naparty, and J. Skoniecsny, J. Phys. C **18**, 2563 (1985).
[14]M. A. Shalaev and B. P. Belinskii, Zh. Tekh. Fiz. **58**, 2360 (1988) [Sov. Phys. Tech. Phys. **33**, 1438 (1988)].
[15]R. Schneider, H. Durr, Th. Fauster, and V. Dose, J. Vac. Sci. Technol. A **8**, 3363 (1990).
[16]V. N. Strocov, H. I. Starnberg, and A. R. H. F. Ettema, Solid State Commun. (to be published).
[17]J.-V. Peetz, W. Schattke, H. Carstensen, R. Manzke, and M. Skibowski, Phys. Rev. B **46**, 10 127 (1992).
[18]E. G. McRae and C. W. Caldwell, Surf. Sci. **57**, 63 (1976).
[19]V. N. Strocov, Int. J. Mod. Phys. B **7**, 2813 (1993).
[20]L. J. Holleboom (private communication).
[21]S. H. Vosko, L. Wilk, and M. Nusair, Can. J. Phys. **58**, 1200 (1980).
[22]J. F. Janak, A. R. Williams, and V. L. Moruzzi, Phys. Rev. B **11**, 1522 (1975).
[23]G. Capart, Surf. Sci. **26**, 429 (1971).
[24]A. Goldmann, W. Altmann, and V. Dose, Solid State Commun. **79**, 511 (1991).